INSTITUTE OF PHYSICS PUBLISHING BIOINSPIRATION & BIOMIMETICS

Bioinsp. Biomim. **1** (2006) 20–29 doi:10.1088/1748-3182/1/1/003

Four flippers or two? Tetrapodal swimming with an aquatic robot

John H Long Jr[1,3], **Joseph Schumacher**[1], **Nicholas Livingston**[1] **and Mathieu Kemp**[2]

[1] Department of Biology, Program in Cognitive Science, and the Interdisciplinary Robotics Research Laboratory, Vassar College, 124 Raymond Avenue, Poughkeepsie, NY 12604, USA
[2] Nekton Research LLC, Durham, NC 27713, USA

E-mail: jolong@vassar.edu

Received 20 January 2006
Accepted for publication 3 April 2006
Published 18 April 2006
Online at stacks.iop.org/BB/1/20

Abstract
To understand how to modulate the behavior of underwater swimmers propelled by multiple appendages, we conducted surge maneuver experiments on our biologically-inspired robot, Madeleine. Robot Madeleine is a self-contained, self-propelled underwater vehicle with onboard processor, sensors and power supply. Madeleine's four flippers, oscillating in pitch, can be independently controlled, allowing us to test the impact of flipper phase on performance. We tested eight gaits, four four-flippered and four two-flippered. Gaits were selected to vary the phase, at either 0 or π rad, between flippers on one side, producing a fore–aft interaction, or flippers on opposite sides, producing a port–starboard interaction. During rapid starting, top-speed cruising, and powered stopping, the power draw, linear acceleration and position of Madeleine were measured. Four-flippered gaits produced higher peak start accelerations than two, but did so with added power draw. During cruising, peak speeds did not vary by flipper number, but power consumption was double in four flippers compared to that of two flippers. Cost of transport (J N^{-1} m^{-1}) was lower for two-flippered gaits and compares favorably with that of aquatic tetrapods. Two four-flippered gaits produce the highest surge scope, a measure of the difference in peak forward and reverse acceleration. Thus four flippers produce superior surge behavior but do so at high cost; two flippers serve well for lost-cost cruising.

1. Introduction

Moving beyond traditional animal experiments and computer simulations, biologists are testing locomotor hypotheses using biomimetic mechanical models (Dickson and Dickinson 2004, Ellington *et al*. 1996, McHenry *et al*. 1995, Sane and Dickinson 2001) and robots (Altendorfer *et al*. 2001, Krieger *et al*. 2000, Long *et al*. 2003, 2004; for review, see Webb (2001, 2002)). Mobile robots built with a few carefully chosen biological features can elucidate the basis of seemingly complex behaviors (Braitenberg 1984) and complement the 'New Robotics' movement, which seeks explicitly to employ bioinspiration in the creation of adaptive behavior in robotic agents (Pfeifer *et al*. 2005). Inspired by the evolutionary transformations of terrestrial to aquatic tetrapods posited by Fish (1996, 1998, 2001), we have developed a remotely-operated robot, Madeleine, to test biological hypotheses about the modulation of locomotor behaviors in swimmers using four lift-based appendages or flippers (Kemp *et al*. 2005, Hobson *et al*. 2005). Our robot differs from a similar four-flipper design suggested by Licht *et al*. (2004) in at least three important ways: (1) the flippers oscillate only in pitch, (2) the flippers, or, in engineering terms, flapping foils, are based on a patented design (Pell 2001), and (3) the robot logs, in addition to acceleration, power draw during swimming. Our goal is to use the four-flippered Madeleine to understand how flippers interact to modulate swimming performance in a self-propelled swimmer.

We are compelled to investigate the interactions of flippers by two observations about tetrapodal lift-based swimmers

---

[3] Author to whom correspondence should be addressed.

(Fish 1996, 2001, 2004, Thewissen and Fish 1997): (1) living aquatic tetrapods that swim using lift-based appendages (e.g., penguins, auks, sea turtles, seals, sea lions, dolphins and whales) do so using either pectoral or pelvic limbs, but not both, for propulsion during steady, straight-line swimming. This is determined by direct observation and by the presence of asymmetric anatomical specializations for propulsive and maneuvering limbs. (2) Some extinct aquatic tetrapods that appear to have swum using lift-based appendages (e.g., plesiosaurs, kronosaurs) did so using all four appendages (for review, see Carroll (1988)). This is determined in plesiosaurs by the presence of hydrofoil-shaped appendages, a flexible trailing edge, and the requisite joint mobility and muscle attachment sites (Reiss and Frey 1991). Given the species richness of the Mesozoic radiation of tetrapods with apparent four-flippered propulsion, why do more recently derived aquatic tetropods use only two limbs for propulsion? Which permits better swimming performance, four flippers or two?

On the basis of work in animals, engineering and robotic systems (Anderson and Kerrebrock 1997, Anderson *et al.* 1998, Bartol *et al.* 2002, Birch and Dickinson 2003, Drucker and Lauder 2001, Fish *et al.* 2003, Lauder *et al.* 2002, Liao *et al.* 2003, Maybury and Lehmann 2004, Standen and Lauder 2005, Triantafyllou *et al.* 1993, 2002, 2004, Walker 2004, Walker and Westneat 2000, 2002), we predict that upstream ('fore') and downstream ('aft') flippers will interact physically in constructive or destructive ways during steady swimming, creating a situation in which the additional energy required to flap four flippers is or is not rewarded with a proportional increase in speed. Specifically, if the fore–aft flipper interactions are constructive, we predict that four-flippered gaits will permit the robot to perform at more than twice the level of two-flippered gaits. For destructive fore–aft interactions, we predict that four-flippered gaits will constrain the robot to perform at less than twice the level of the two-flippered gaits. Neutral fore–aft interactions are purely additive and indicate that the flippers operate without physical interaction. If a constructive or destructive physical interaction is present, its likely mechanism would be the vortex shed by the upstream flipper altering the momentum of the fluid volume encountered by the downstream flipper (Anderson *et al.* 1998, Prandtl and Tietjens 1934, Triantafyllou *et al.* 1993). While Kelvin's theorem of vorticity guarantees the presence of a wake, this study is not designed to detect wakes directly. That task requires flow visualization. However, a physics-based inference for wake interactions could be made if experiments showed that isolated changes in the fore–aft phases of flippers altered the robot's swimming performance.

For flippers located on opposite sides of the body, we predict a physical interaction of their roll moments, where roll is rotation about the robot's long axis. Roll moments counter-balance when left–right flipper pairs ('port–starboard' interaction) oscillate in phase, stabilizing the robot in roll and thus, we predict, enhancing swimming performance compared to when the flippers operate in anti-phase (one-half cycle, 180°, or π rad). With flippers in anti-phase, we recognize that the ensuing body roll will add heave motion to the pitching flippers, a situation that will alter the governing hydrodynamics and potentially produce unanticipated thrust performance (Schouveiler *et al.* 2005).

2. Methods

2.1. Robot design

While details specific (Kemp *et al.* 2005) and general (Hobson *et al.* 2005) of robot Madeleine's design can be found elsewhere, we briefly recapitulate features important to this project. Foremost, Madeleine has a number of biologically-inspired features (figure 1): (1) a four-flippered, bilaterally-symmetric, tetrapod-like architecture, (2) flippers (Pell 2001) with Young's modulus, 0.9 MPa, similar to that found in vertebrate bodies (Koob and Long 2000, Summers and Long 2006), (3) flippers that work using an oscillating vortex-shedding mechanism (Koochesfahani 1989, Sarkar and Venkatraman 2006, Terada and Yamamoto 2004) that likely shares underlying hydromechanical principles with the flapping forelimbs of sea turtles (Wyneken 1997), (4) the flippers are under independent control and can be coordinated in multiple patterns, (5) and overall length (0.78 m stem to stern) and weight (24.4 kg dry, including flippers of 1.1 kg each) of Kemp's and olive Ridley sea turtles (Spotila 2004), and, perhaps most importantly, (6) a power density of 5 W kg^{-1} during cruising (100 W total) and 10 W kg^{-1} during acceleration (200 W total) that is similar to that found in vertebrate aerobic muscle (Alexander 1999).

We caution, however, that Madeleine is not bioinspired in the following features: (1) the flippers actuate in pitch only, with single-degree-of-freedom control, (2) the flippers have a standard foil shape, the NACA profile 0017 with 2.4 cm thickness 4.0 cm from the leading edge, and a 15.3 cm span and chord, and (3) the robot's buoyancy is neutral and invariant.

The flippers were driven by 70 W brushed motors (Maxon) that were powered by 6 Å amplifiers (AMC Z-series) and controlled by a four-axis motion controller (Galil). The onboard processor was a PC104 (Transmetta Crusoe; 533 MHz), running embedded Windows XP, with data from sensors logged on a 512 Mb flash device, and serving a top-side laptop client for remote control via a wireless (RF) joystick (Saitek). Onboard sensors included a dynamical measurement unit (Microstrain 3DM-GX1) that measured the robot's pitch and linear acceleration. Power draw was recorded as the product of the instantaneous voltage drop at the battery and the current, as measured by a calibrated, precision current sense amplifier (Linear Technology LT1878).

Advantages of using robots for hypothesis testing are that (1) particular features can be studied in isolation from covarying features found in nature, (2) system inputs (energy, control algorithms) can be directly monitored and compared to performance outputs (acceleration, speed) and (3) behavior can be predetermined. Notable disadvantages of using robots include (1) isolation of certain features in the robot assumes that those features operate in life independently from other, omitted features, (2) predetermination of robotic behavior eliminates the opportunity to observe the unanticipated, and

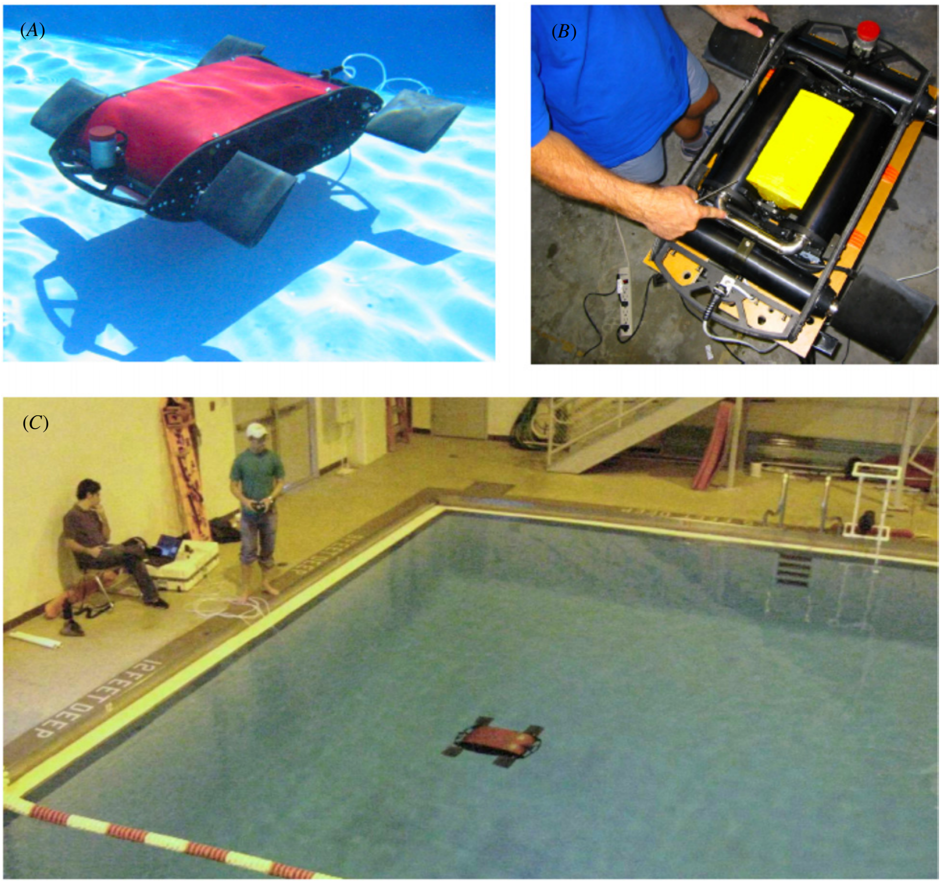

Figure 1. Madeleine, a biomimetic, aquatic, robotic tetrapod. (A) Swimming in outdoor pool with all flippers in phase, gait [(0, 0), (0, 0)] (see figure 2). Flippers oscillate in pitch. Note aft tether for remote operation. (B) Swim skin removed, showing waterproof bottles housing servo motors fore and aft, and, amidships, computer, sensors and batteries. (C) Experiments in dive well, with Madeleine swimming at 1 m depth, controlled by an operator (white cap), monitored via a computer (seated person), and filmed by an underwater video camera (white frame next to pool ladder).

(3) constancy of robotic form and function explores less of the possible parameter space naturally sampled by biological variants.

2.2. Operating parameters

The robot Madeleine operated in freshwater at temperatures of 20 to 21 °C. In all experiments, the flippers oscillated at 6 Hz with a pitch amplitude of 20°. Since the grand mean of peak forward steady cruising speed for all trials (results detailed below) was 0.71 $\mathrm{m\ s^{-1}}$, we used that value to calculate the following scaling parameters: Strouhal number of the flippers was 0.38, advance ratio of the flippers was 1.08, and Reynolds number of the robot was 101 145.

2.3. Experiments

We tested and compared eight gaits: four used four flippers and four used two (figure 2). When two flippers were used for propulsion, we left in place the other two flippers, which were held rigidly in a horizontal posture. In spite of the fact that animals that rely on two flippers tend to show enlargement of the propulsive pair or reduction of the non-propulsive, we kept non-propulsive pairs in place for three reasons, all related to possible experimental artifacts relative to the intended investigation of differences caused by gait alone: (1) flipper removal reduces the robot's drag, increasing swimming speed, (2) flipper removal reduces the robot's mass, improving acceleration performance and (3) flipper removal alters the robot's passive trim and dynamic stability.

Experiments were conducted in the 3 m deep diving well of the pool at Vassar College (figure 1(C)). For all tests, a diver placed Madeleine at a depth of 1 m with the 15 m tether coiled to provide slack for the distance of the trial. For all gaits, all propulsive flippers were oriented initially with tips pointed vertically up. At a signal from the diver, the topside operator engaged Madeleine, with a single control, at full power and in a straight line forward. After Madeleine had translated at least two body lengths—a distance we had predetermined was sufficient to reach a constant, steady, and top cruising speed—the operator engaged full reverse power, which was sustained until Madeleine had achieved constant reverse speed (figure 3). Battery voltage was monitored continuously and trials were discarded and discontinued if peak power draws

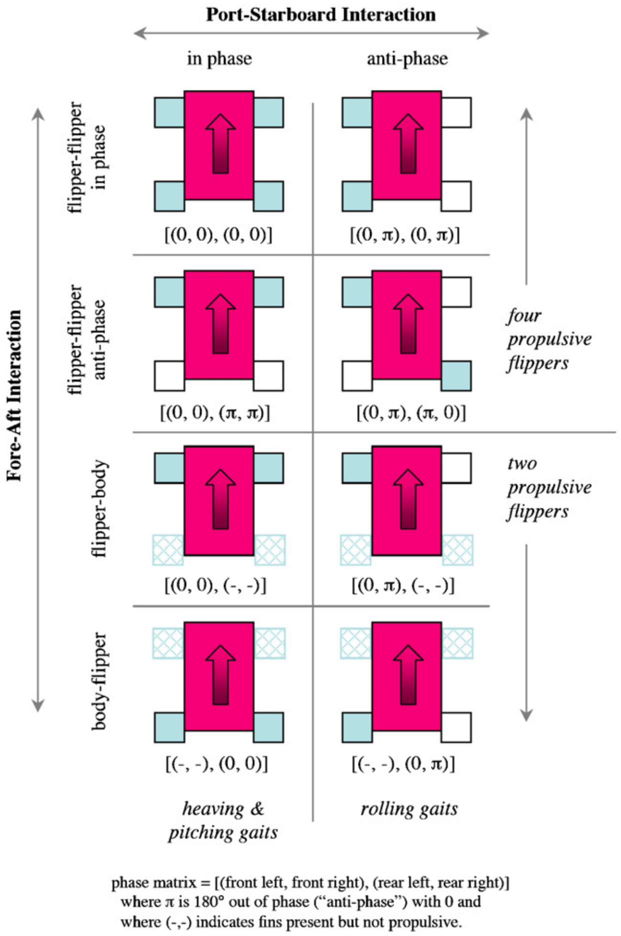

Figure 2. Gaits and flipper interactions. In fore–aft interactions, two flippers on one side are oscillating either in phase or anti-phase; in the two-flipper gaits, the fore–aft interactions are between the upstream flipper and body ('flipper-body') or body and downstream flipper ('body-flipper'), where the stationary flipper is considered to be part of the body. Port–starboard interactions characterize left–right flipper phases. Eight gaits are uniquely defined as indicated by the phase matrix for each. Flippers of the same color operate in–phase; flippers of different colors operate in anti-phase. Muted, cross-hatched flippers are kept in place during experiments but are not propulsive. Each gait was tested three times in a random order ($n = 24$).

dropped voltage below 10 V_{dc}. Motor temperatures were also monitored continuously and trials were discarded and discontinued if temperatures immediately following operation exceeded 40 °C; temperatures often transiently exceeded 40 °C during a trial. High-frequency noise in the temperature sensor precluded its use as an event-based response variable.

We sampled three kinds of performance information with three different sensor systems: (1) total power draw (in W; 5 Hz temporal resolution; 0.2 W power resolution), (2) forward and reverse acceleration (in m s^{-2}; 5 Hz temporal resolution; 0.01 m s^{-2} acceleration resolution) and (3) displacement (in m; 30 Hz temporal resolution; 0.0025 m spatial resolution) with an external submerged video system (Panasonic model AG-1960, SVHS). We created response variables that characterized both acceleration and top-speed cruising (figure 3): peak start power, mean cruise power and peak stop power; peak start acceleration, peak stop acceleration; start time (to translate one body length), peak steady cruising speed and distance to stop. Note that start time and distance to stop are related to peak start and peak stop acceleration; however, the former variables are complementary rather than duplicative since they integrate acceleration over time while the latter pair measures near-instantaneous acceleration.

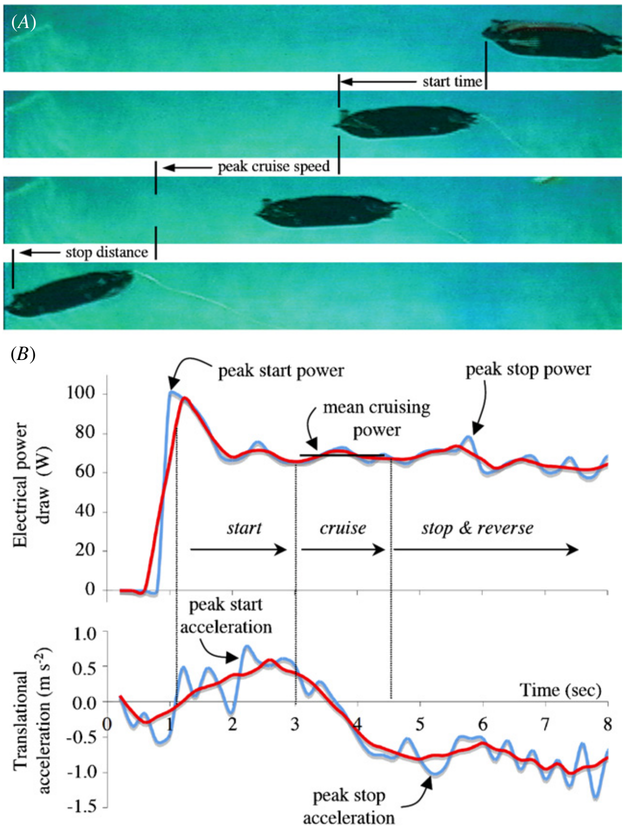

Figure 3. Experimental response variables. Sample data from a four-flippered trial, gait [(0, π), (0, π)], with a peak cruising speed of 0.71 m s^{-1}. (A) Kinematic variables measured from an underwater video. (B) Power draw and translational acceleration from on-board sensors. Acceleration corrected for gravitational acceleration. Blue lines are raw data; red lines are low-pass filtered. Raw data used for measurements.

Each gait was tested five times, with the order of the 40 trials randomized. Occasional system or operator errors allowed us to only use three of the five trials for some gaits, so we used three replicates across all gaits for a sample size of 24. This testing process was repeated twice, once for the trials in which video was recorded and again for logging of acceleration and power draw. These trials were segregated because of the need to coordinate multiple personnel.

2.4. Data analysis

Files containing the power and acceleration data were downloaded from Madeleine following each trial. Unfiltered data were used to find power draws; the hotel or resting power draw was also measured and was constant at 24.65 W (±0.463, 1 st. error) across all trials, as determined by ANOVA. Peak and cruising power draws excluded the hotel load. Raw forward–backward acceleration data were corrected using trigonometry for the pitch of the robot, since any pitch out of the horizontal plane induces an apparent increase in forward acceleration due to gravity. Data were otherwise unfiltered.

Video records were converted into QuickTime movies (iMovie software, Apple Computer) and analyzed frame-by-frame (VideoPoint software, Lennox Softworks). We manually tracked the cylindrical bowsprit of the robot (see figure 3).

2.5. Statistical analysis

In order to compare the influence of the fore–aft and the port–starboard interactions, we conducted a two-way fully factorial ANOVA (JMP statistical software, version 5.0). We planned three *a priori* contrasts for the fore–aft interaction factor: (1) four- *versus* two-flippered gaits, (2) within four-flippered gaits, in-phase *versus* anti-phase gaits, and (3) within two-flippered gaits, in-phase *versus* anti-phase gaits. The significance level, α, for probability was 0.05; marginally significant effects were $0.05 < \alpha < 0.10$. Note that if gaits *per se* are important, we would see, in combination, significance for all the aforementioned contrasts and the port–starboard interaction.

2.6. Compound performance metrics

In order to compare robot Madeleine's performance to that of aquatic tetrapods swimming submerged, we calculated the dimensionless cost of transport, CT:

$$\mathrm{CT} = \frac{P}{UMg} \tag{1}$$

where P is the metabolic or, in our case, electrical power (W), U is the steady swimming speed (m s^{-1}), M is the dry body mass (kg), and g is the gravitational acceleration (m s^{-2}) (Videler and Nolet 1990). CT values for robot Madeleine used total power draw during cruising, including the hotel load, analogous to the basal metabolic rate measured by respirometry in animals.

Since CT accounts for steady, constant-velocity performance, we sought a metric for unsteady linear maneuvering; we derived the surge scope, SS. Surge is the forward and reverse acceleration along the vehicle's or animal's trajectory, and is important in docking, formation swimming, and station-holding (Webb 2004). We calculate SS as follows:

$$\mathrm{SS} = \frac{a_{\mathrm{forward}} - a_{\mathrm{reverse}}}{g} = \frac{\Delta a}{g} \tag{2}$$

where a_{forward} and a_{reverse} are the peak accelerations measured during starting and stopping, respectively. This dimensionless number can also be understood as the ratio of the difference in peak forward and reverse thrust (N) to the weight of the swimmer (N); body mass (kg) cancels out to yield the mass-independent formulation given in equation (2).

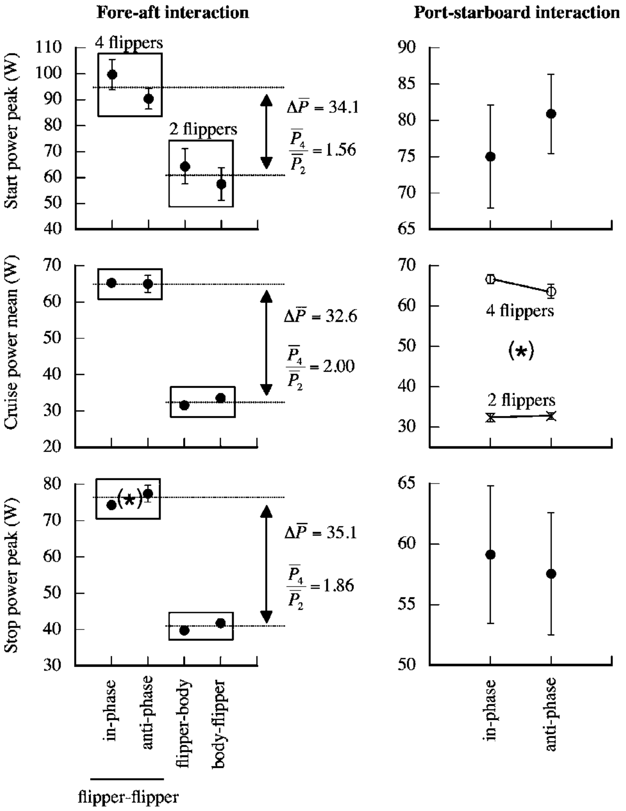

Figure 4. Power draw as a function of fore–aft interaction, flipper number and port–starboard interaction. Means ± one standard error. Means in different boxes are statistically distinct ($p < 0.05$) in *a priori* contrasts. Asterisks in parentheses denote marginal significance ($0.05 < p < 0.10$). Means connected by lines denote an interaction effect (fore–aft × port–starboard). For start power peak, two-way ANOVA significant ($n = 24$, $r^2 = 0.767$, F ratio = 7.5, MSE = 154.2, $p = 0.0004$). For cruise power mean, two-way ANOVA significant ($n = 24$, $r^2 = 0.981$, F ratio = 119.5, MSE = 7.7, $p < 0.0001$). For stop power peak, two-way ANOVA significant ($n = 24$, $r^2 = 0.983$, F ratio = 131.3, MSE = 130.3, $p < 0.0001$).

3. Results

For the fore–aft interaction, the power draw of four- and two-flippered gaits differed significantly during start, cruise and stop, with four-flippered gaits drawing 56 to 100% more power (figure 4). The 100% increase in power draw for cruising shows a neutral interaction of fore and aft flippers. The smaller increases of 56 and 86% for starting and stopping, respectively, demonstrate either constructive interactions or the presence of asynchronous power draw for anti-phase gaits. We regard the latter possibility as unlikely given the fact that *a priori* contrasts detected no significant increase in power draw within four-flippered gaits as a function of in-phase motor action; moreover, a marginally-significant difference occurs in the opposite direction for the stop power draw. A marginal significance was detected in cruise power as a statistical interaction between the fore–aft and port–starboard effects, with four-flippered gaits having lower cruise power draw in port–starboard anti-phase and two-flippered gaits having the

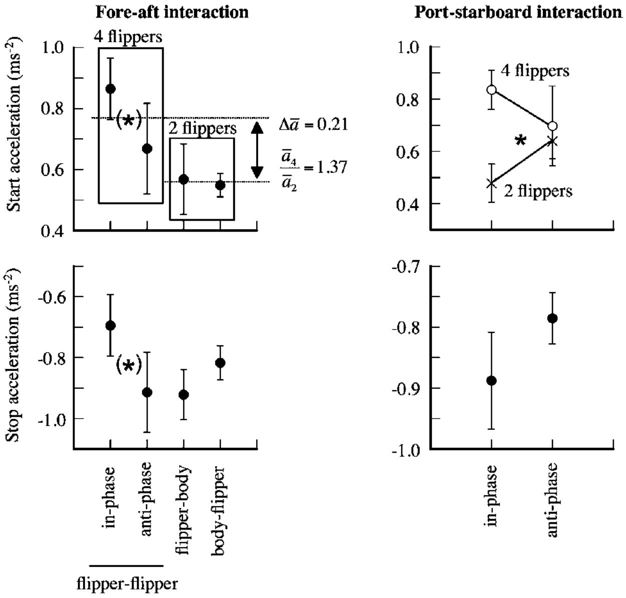

Figure 5. Acceleration as a function of fore–aft interaction, flipper number, and port–starboard interaction. Means ± one standard error. Means in different boxes are statistically distinct ($p < 0.05$) in *a priori* contrasts. Asterisks in parentheses and without denote marginal significance ($0.05 < p < 0.10$) and significance ($p < 0.05$), respectively, between means. Means connected by line denotes an interaction effect (fore–aft × port–starboard). For start acceleration peak, two-way ANOVA significant ($n = 24$, $r^2 = 0.704$, F ratio = 5.4, MSE = 0.00029, $p = 0.0024$). For stop acceleration peak, two-way ANOVA not significant ($n = 24$, $r^2 = 0.415$, F ratio = 1.6, MSE = 0.00041, $p = 0.199$).

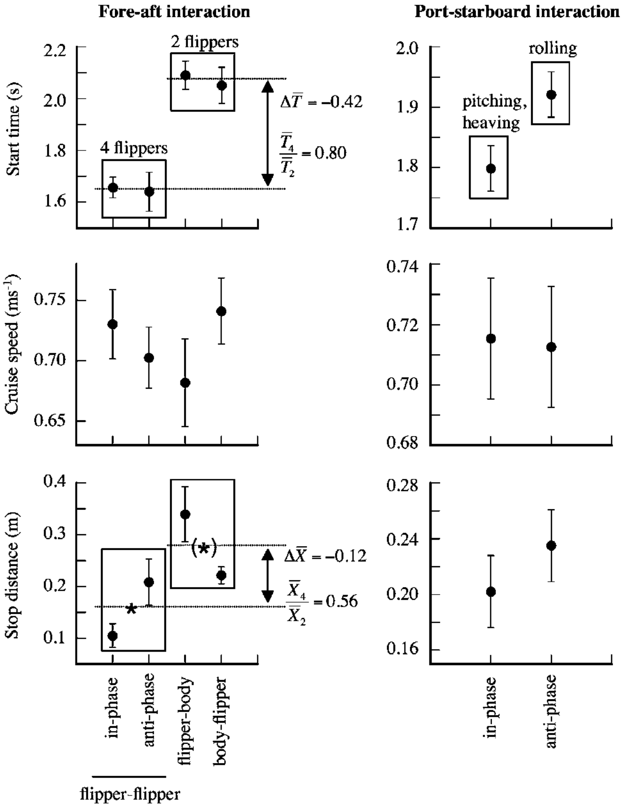

Figure 6. Kinematic features as a function of fore–aft interaction, flipper number and port–starboard interaction. Means ± one standard error. Means in different boxes are statistically distinct ($p < 0.05$) in *a priori* contrasts. Asterisks in parentheses and without denote marginal significance ($0.05 < p < 0.10$) and significance ($p < 0.05$), respectively, between means. For start time, two-way ANOVA significant ($n = 24$, $r^2 = 0.813$, F ratio = 10.0, MSE = 0.0170, $p < 0.0001$). For cruise speed, two-way ANOVA not significant ($n = 24$, $r^2 = 0.220$, F ratio = 0.6, MSE = 0.0049, $p = 0.714$). For stop distance, two-way ANOVA significant ($n = 24$, $r^2 = 0.579$, F ratio = 3.1, MSE = 0.008, $p = 0.028$).

opposite trend. This suggests that any rolling moment caused by port–starboard anti-phase flipper motion is costly for two-flippered gaits but is either counter-balanced, in the case of the [(0, π), (π, 0)] gait, or exaggerated, in the case of the [(0, π), (0, π)] gait, to positive effect. Please note that we did not measure vehicle roll directly.

For the fore–aft interaction, peak acceleration of four- and two-flippered gaits differed significantly during starts, with four-flippered gaits producing accelerations 37% greater (figure 5). That accelerations of four-flippered gaits were not 100% or more greater, or were not different for stop accelerations, for four-flippered gaits refutes the hypothesis that the flippers would interact constructively. During start and stop the in-phase four-flippered gaits had, respectively, marginally higher positive and lower negative accelerations than the anti-phase four-flippered gaits. This marginal significance is the only difference for any of the stop acceleration contrasts; thus, stop acceleration does not differ by number of flippers. For the port–starboard interaction, a significant fore–aft × port–starboard statistical interaction exists for the start acceleration, with four-flippered gaits decreasing acceleration from in-phase to anti-phase and two-flippered fins showing the opposite trend. Further, even though four-flippered gaits out-perform two flippered gaits in terms of start acceleration, they do so by drawing more power (56%, see figure 4) than is returned as peak acceleration (37%). Also, the additional 86% increase in power draw peak during stopping (see figure 4) does not produce a difference between four- and two-flippered gaits.

For the fore–aft interaction, start time and stop distance of four- and two-flippered gaits differed significantly, with four-flippered gaits starting in 20% less time and stopping in 44% less distance (figure 6). The 20% decrease in start time is less than the 50% or more expected by constructive flipper interactions. The nearly 50% decrease in stop distance is close to that expected for neutral (additive) flipper interactions. No significant differences exist among the gaits for cruise speed, supporting the destructive interaction hypothesis. For the port–starboard interaction, start time decreased significantly for those gaits with flipper pairs in-phase compared to those in anti-phase.

Relative to the cost of transport, CT, of submerged tetrapods, robot Madeleine compares favorably, with her two-flippered gaits producing CTs between 0.3 and 0.4, a range also occupied by the two-flippered sea turtles and harbor seals and encompassed by California sea lions (figure 7(A)).

Even Madeleine's more power-consumptive four-flippered gaits have lower CTs than some penguins and beaver.

Not all four-flippered gaits are equivalent in terms of performance. When we examine the CT, a steady-swimming metric, in combination with surge scope, SS, a metric of unsteady performance (see equation (2)), we see that the $[(0, \pi), (0, \pi)]$ and $[(0, 0), (\pi, \pi)]$ gaits produce the highest SS of all. Two-flippered gaits produce intermediate SS and have the lowest CT.

4. Discussion

Four flippers or two? The answer depends on the situation. If power consumption is no object, then four flippers outperform two during starting and stopping (figures 5 and 6). For robot Madeleine, this may be a reasonable trade-off for these transient surge maneuvers. During cruising, however, power consumption matters if one cares about mission time, and in this situation two flippers produce the same peak speed at half the cost (figure 6). Thus designers and builders of biomimetic, aquatic, robotic tetrapods would be well advised to use sequential gait transitions in even simple surge and cruise maneuvers. Or, if design or mission constraints warrant a single gait, two-flippered gaits are superior as a group, yielding the lowest cost of transport, CT, and intermediate surge performance, SS (figure 7).

In submerged vertebrates, our understanding of swimming maneuvers has been limited because of the difficulty in getting animals to vary and repeat their behavior in experimental situations (Webb 2006). Behavior can be varied and replicated in biomimetic swimmers, such as robot Madeleine, and, with a variety of performance measures from external and internal sensors, we are beginning to gain insight into underlying mechanisms.

We investigated three translational surge maneuvers: (1) starting quickly, (2) stopping quickly and (3) cruising at peak speed. To maximize starting, four-flippered gaits with fore–aft flippers in phase, $[(0, \pi), (0, \pi)]$ and $[(0, 0), (0, 0)]$, produce greater peak accelerations than the anti-phase four-flippered gaits and the two-flippered gaits (figures 5 and 7). In addition, within the four-flippered group, in-phase coordination of the port–starboard flippers maximizes starting acceleration (figure 5). Moreover, we see the same pattern in the start time, the time to accelerate the robot one body length, with four flippers and port–starboard in-phase gaits generating the shortest acceleration time (figure 6). Taken in combination, these results identify the $[(0, 0), (0, 0)]$ gait, with all four flippers operating in phase, as the best at maximizing peak starting acceleration. Because robot Madeleine starts from rest in still water, for this maneuver the physical interaction of the flippers cannot be mediated by flow interactions. Instead, flipper phase itself is the key control parameter. Simply, we interpret the results to indicate that the instantaneous thrust produced by all four flippers operating independently and in-phase sum to produce the largest possible peak thrust forces and hence greater peak accelerations.

At first glance, stopping is the surge maneuver that is more likely than starting to show evidence of wake-mediated fore–aft flipper interactions, since the robot's downstream flippers move through a fluid volume into which momentum has been injected by the active (four-flippered gaits) or passive (two-flippered gaits) body. In contrast to the start, the peak acceleration for stopping is least for the in-phase, four-flippered gaits, while the other gaits reach peak values nearly equal and opposite to the those seen in the in-phase, four-flippered gaits during starting (figure 5). However, even without greater peak stop accelerations, the in-phase, four-flippered gaits manage to stop in the shortest distance (figure 6). While it might be that the in-phase, four-flippered gaits are able to transfer more kinetic energy to the fluid during the entire stopping period, that possibility is not reflected in either the peak electric power draw values (figure 4) or in the robot pitching (up to −20° relative to cruising pitch but not different among gaits) as it brakes (see figure 3; pitch measured

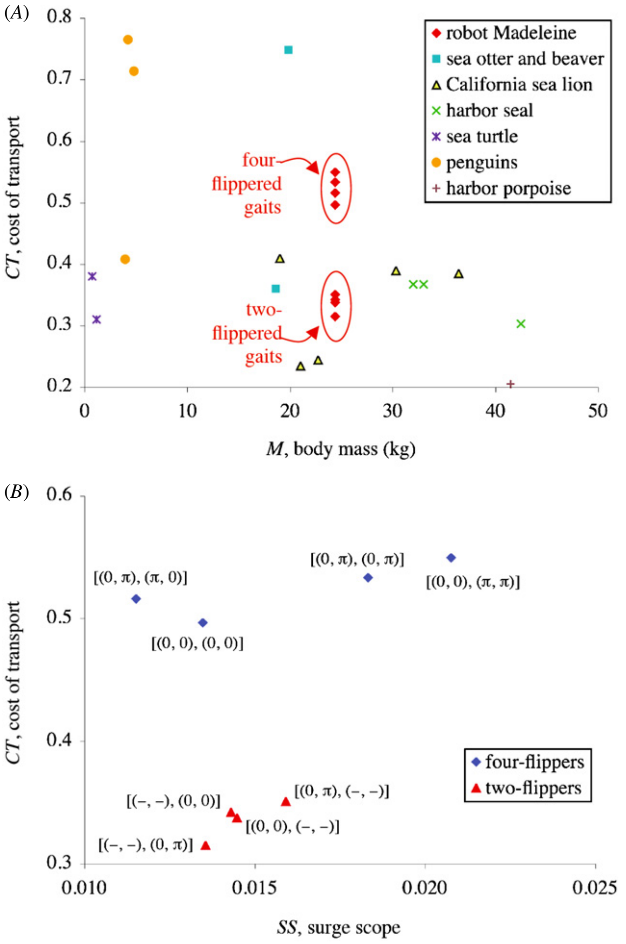

Figure 7. Performance metrics of robot Madeleine. (A) Cost of transport, CT, of robotic and biologic aquatic tetrapods (see equation (1)). Sea otter and beaver values are for submerged swimming; neither uses lift-based flippers. All other animals use lift-based flippers. Data for animals from Fish *et al*. (2000). (B) CT and surge scope, SS, of robot Madeleine characterize, respectively, steady and unsteady translational swimming performance. Two four-flippered gaits (for explanation of phase matrices see figure 2) are the poorest performers, with a high CT and low SS. All of the two-flippered gaits are good compromises of low CT and intermediate SS.

for acceleration correction but not reported; see section 2). Thus it is impossible here to infer a single physical mechanism for stopping without direct flow visualization.

Cruising at peak speed is a translational surge maneuver characterized by low accelerations and a nearly constant power draw for a particular gait (see figure 3). Because cruising at a constant velocity is ideally a steady-state phenomenon, the robot-fluid system has time, in contrast to transient starting and stopping, to develop the wake-mediated fore–aft flipper interactions, if they exist. Most telling in this regard is that the peak cruise speeds among gaits were statistically indistinguishable (figure 6), in spite of the fact that four-flippered gaits used exactly twice as much power as the two-flippered (figure 4). Thus, in terms of energy usage, four-flippered gaits are only half as efficient as two-flippered. This begs the question: how is that extra energy being dissipated? As has been experimentally demonstrated (Triantafyllou *et al.* 1993), an oscillating hydrofoil encountering a vortex wake responds in three ways, depending on how it intersects the momentum field. The vortex wake may (1) enhance hydrofoil thrust by adding to its circulation, (2) reduce hydrofoil thrust by subtracting from its circulation, or (3) leave hydrofoil thrust unchanged by a combination of momentum addition and subtraction. Timing is the key: alter slightly the movement of the hydrofoil into the vortex and drastic changes are possible. This hydromechanical behavior is the basis for the 'vorticity control' approach to modulating fish-like propulsion and maneuverability (Anderson and Kerrebrock 1997, Anderson *et al.* 1998, Bandyopadhyay 2005, Triantafyllou *et al.* 2002). Within that paradigm, our results for peak cruising speeds are consistent with the interpretation that the four-flippered gaits tested here suffer from destructive wake interactions.

Still left to investigate is the generality of these results. Do they apply to all multi-appendage vehicles, or just to ones with similar architectures and operating parameters? We can investigate this question, in part, using robot Madeleine and varying flipper operation parameters, flipper shape and material, and range of maneuvers. Moreover, even with the identical experimental conditions of this study, we have only investigated a small fraction of the possible phase space for the flipper interactions. Specifically, given the importance of even small differences in phase to the mechanical performance of foils in fluid (Fish *et al.* 2000, 2003, Gordon *et al.* 2001, Maybury and Lehmann 2004, Sane and Dickinson 2001), the vorticity control paradigm predicts that constructive wake interactions are likely to occupy only a small portion of the parameter space and we are unlikely to have found those constructive 'sweet spots' with only two fore–aft flipper phases, in-phase and anti-phase.

Relating the results of this study to the physiology of aquatic animals must be done with extreme caution. We agree with and follow Webb (2001), who argues that robots and computer programs co-exist as simulation models and, as such, are subject to similar constraints and limitations. To provide predictive insight into biological systems, both robotic and computer models need to explicitly address their relevance, level, generality, abstraction, accuracy, behavioral match and physical basis (Webb 2001). We designed and built robot Madeleine (Kemp *et al.* 2005) to test biological hypotheses about swimming gaits and wake interactions at the level of an individual swimmer; as discussed above, robot Madeleine addresses general issues faced by both multi-appendage vehicles and animals and does so, on the advice of Webb (2001), by simplification rather than idealization; accuracy, behavioral match and physical basis are best seen by the animal-like features such as bilateral symmetry and flipper-based propulsion (figure 1), physiological power density and performance equivalent to that of real aquatic tetrapods (figure 7(A)).

Until a better model simulation is produced, we argue that robot Madeleine is the best available, according to Webb's seven criteria (2001), to address biological questions about multi-appendage swimming. For example, these experimental results suggest that the plesiosaurs, bearing four putatively-propulsive flippers (Carroll 1988), were likely to have been ambush predators, taking advantage of the better acceleration of four flippers over two. If they did cruise routinely, then our results suggest that they either did so using only one pair of flippers at a time or with four-flippers under circumstances when they were not energy limited. Moreover, extant fully-aquatic tetrapods cruise with only two flippers, and our results suggest that a lower CT is the reason. The flippers not used for propulsion are free to be co-opted as control surfaces for enhanced maneuvers (Fish 1998, 2004). Finally, the evolutionary transition from four-footed, drag-based paddling to two-flippered lift-based subaqueous flying may be facilitated by the destructive wake interactions suggested here; many facultative tetrapod swimmers use only a pair of feet to paddle at times (Fish 1998). If nothing else, the generation of physically-based predictions about animal behavior is one purpose served by robot Madeleine.

Acknowledgments

The robot development project was funded by a National Science Foundation grant to JHL (BCS-0320764) and by internal R & D funds at Nekton Research LLC. The experiments at Vassar College would not have been possible without the help of Jesup Szatkowski, Keon Combie, Virginia Engel, Kira Irving, Jessie Kates. Madeleine Long, Isabel Long and Adele Long were inspirational. Finally, we thank Charles Pell, Brett Hobson, and John Keller for help designing, building, and testing robot Madeleine. Experiments were funded by a National Science Foundation grant to JHL (DBI-0442269).

References

Alexander R M 1999 *Energy for Animal Life* (New York: Oxford University Press)

Altendorfer R, Moore N, Komsuoglu H, Buehler M, Brown H B Jr, McMordie D, Saranli U, Full R and Koditschek D E 2001 RHex: a biologically inspired hexapod runner *Auton. Robots* **11** 207–13

Anderson J M and Kerrebrock P A 1997 The vorticity control unmanned undersea vehicle (VCUUV)—an autonomous vehicle employing fish swimming propulsion and maneuvering *Proc. 10th Int. Symp. Unmanned Untethered Submersible Technology (Autonomous Undersea Systems Institute, Lee, NH)*

Anderson J M, Streitlien K, Barrett D S and Triantafyllou M S 1998 Oscillating foils of high propulsive efficiency *J. Fluid Mech.* **360** 41–72

Bandyopadhyay P R 2005 Trends in biorobotic autonomous undersea vehicles *IEEE J. Ocean. Eng.* **30** 109–39

Bartol I K, Gordon M S, Gharib M, Hove J R, Webb P W and Weihs D 2002 Flow pattern around the carapaces of rigid-bodied, multi-propulsor boxfishes (Teleostei: Ostraciidae) *Integr. Comput. Biol.* **42** 971–80

Birch J M and Dickinson M H 2003 The influence of wing-wake interactions on the production of aerodynamic forces in flapping flight *J. Exp. Biol.* **206** 2257–72

Braitenberg V 1984 *Vehicles: Experiments in Synthetic Psychology* (Cambridge, MA: MIT Press)

Carroll R L 1988 *Vertebrate Paleontology and Evolution* (New York: Freeman)

Dickson W B and Dickinson M H 2004 The effect of advance ratio on the aerodynamics of revolving wings *J. Exp. Biol.* **207** 4269–81

Drucker E and Lauder G 2001 Locomotor function of the dorsal fin in teleost fishes: experimental analysis of wake forces in sunfish *J. Exp. Biol.* **204** 2943–58

Ellington C P, vanden Berg C, Willmot A P and Thomas A L R 1996 Leading-edge vortices in insect flight *Nature* **384** 626–30

Fish F E 1996 Transitions from drag-based to lift-based propulsion in mammalian aquatic swimming *Am. Zoologist* **36** 628–41

Fish F E 1998 Biomechanical perspective on the origin of cetacean flukes *The Emergence of Whales: Evolutionary Patterns in the Origin of Cetacea* ed J G M Thewissen (New York: Plenum) pp 303–24

Fish F E 2001 Mechanism for evolutionary transition in swimming mode by mammals *Secondary Adaptation of Tetrapods to Life in Water* ed J-M Mazin, P Vignaud and V de Buffrenil (New York: Verlag Dr Friedrich Pfeil) pp 261–87

Fish F E 2004 Structure and mechanics of nonpiscine control surfaces *IEEE J. Ocean. Eng.* **29** 605–21

Fish F E, Peacock J E and Rohr J 2000 Phase relationships between body components of odontocete cetaceans in relation to stability and propulsive mechanisms *Proc. 1st Int. Symp. on Aqua Bio-Mechanisms/International Seminar on Aqua Bio-Mechanisms (Tokai University Pacific Center, Honolulu, Hawaii)* ed N Kato and Y Suzuki pp 57–60

Fish F E, Peacock J E and Rohr J J 2003 Stabilization mechanism in swimming odontocete cetaceans by phased movements *Mar. Mammal Sci.* **19** 515–28

Gordon M S, Hove J R, Webb P W and Weihs D 2001 Boxfishes as unusually well controlled autonomous underwater vehicles *Physiol. Biochem. Zool.* **73** 663–71

Hobson B W, Kemp M, Moody R, Pell C A and Vosburgh F 2005 Amphibious robot devices and related methods *US Patent* 6,974,356

Kemp M, Hobson B and Long J H Jr 2005 Madeleine: an agile AUV propelled by flexible fins *Proc. 14th Int. Symp. Unmanned Untethered Submersible Technology (UUST) (Autonomous Undersea Systems Institute, Lee, NH)*

Koochesfahani M M 1989 Vortical patterns in the wake of an oscillating airfoil *AIAA J.* **27** 1200–5

Krieger M J B, Billeter J B and Keller L 2000 Ant-like task allocation and recruitment in cooperative robots *Nature* **406** 992–5

Liao J C, Beal D N, Lauder G V and Triantafyllou M S 2003 The Karman gait: novel body kinematics of rainbow trout swimming in a vortex street *J. Exp. Biol.* **206** 1059–73

Licht S, Polidoro V, Flores M, Hover F S and Triantafyllou M S 2004 Design and projected performance of a flapping foil AUV *IEEE J. Ocean. Eng.* **29** 786–94

Long J H Jr, Lammert A C, Pell C A, Kemp M, Strother J, Crenshaw H C and McHenry M J 2004 A navigational primitive: biorobotic implementation of cycloptic helical klinotaxis in planar motion *IEEE J. Ocean. Eng.* **29** 795–806

Long J H Jr, Lammert A C, Strother J and McHenry M J 2003 Biologically-inspired control of perception-action systems: helical klinotaxis in 2D robots *Proc. 13th Int. Symp. Unmanned Untethered Submersible Technology (UUST) (Autonomous Undersea Systems Institute, Lee, NH)*

Low K H and Willy A 2005 Development and initial investigation of NTU robotic fish with modular flexible fins *IEEE Int. Conf. Mechatronic & Automation, ICMA 2005* pp 958–63

Maybury W J and Lehmann F O 2004 The fluid dynamics of flight control by kinematic phase lag variation between two robotic insect wings *J. Exp. Biol.* **207** 4707–26

McHenry M J, Pell C A and Long J H Jr 1995 Mechanical control of swimming speed: stiffness and axial wave form in an undulatory fish model *J. Exp. Biol.* **198** 2293–305

Pell C A 2001 Impellers with bladelike elements and compliant tuned transmission shafts and vehicles including same *US Patent* 6,250,585

Pfeifer R, Iida F and Bongard J 2005 New robotics: design principles for intelligent systems *Artif. Life* **11** 99–120

Prandtl L and Tietjens O G 1934 *Applied Hydro- and Aeromechanics* (Toronto: United Engineering Trustees)

Reiss J and Frey E 1991 The evolution of underwater flight and the locomotion of plesiosaurs *Biomechanics in Evolution* ed J M V Rayner and R J Wootton (Cambridge: Society for Experimental Biology) pp 131–44 (*Seminar Series* 36)

Sane S P and Dickinson M H 2001 The control of flight force by a flapping wing: lift and drag production *J. Exp. Biol.* **204** 2607–26

Sarkar S and Venkatraman K 2006 Numerical simulation of thrust generating flow past a pitching airfoil *Comput. Fluids* **35** 16–42

Schouveiler L, Hover F S and Triantafyllou M S 2005 Performance of flapping foil propulsion *J. Fluids Struct.* **20** 949–59

Spotila J R 2004 *Sea Turtles: A Complete Guide to Their Biology, Behavior, and Conservation* (Baltimore, MD: The Johns Hopkins University Press)

Standen E M and Lauder G V 2005 Dorsal and anal fin function in bluegill sunfish *Lepomis macrochirus*: three-dimensional kinematics during propulsion and maneuvering *J. Exp. Biol.* **208** 2753–63

Summers A P and Long J H Jr 2006 Skin and bones, sinew and gristle: the mechanical behavior of fish skeletal tissues *Fish Biomechanics* vol 23 ed R E Shadwick and G V Lauder (New York: Elsevier) pp 141–78 (*Fish Physiology Series*)

Terada Y and Yamamoto I 2004 An animatronic system including lifelike robotic fish *Procs. IEEE* **92** 1814–20

Thewissen J G M and Fish F E 1997 Locomotor evolution in the earliest cetaceans: functional model, modern analogues, and paleontological evidence *Paleobiology* **23** 482–90

Triantafyllou G S, Triantafyllou M S and Grosenbauch M A 1993 Optimal thrust development in oscillating foils with application to fish propulsion *J. Fluids Struct.* **7** 205–24

Triantafyllou M S, Techet A H and Hover F S 2004 Reviews of experimental work in biomimetic foils *IEEE J. Ocean. Eng.* **29** 585–94

Triantafyllou M S, Techet A H, Zhu Q, Beal D N, Hover F S and Yue D K P 2002 Vorticity control in fish-like propulsion and maneuvering *Integr. Comput. Biol.* **42** 1026–31

Videler J J and Nolet B A 1990 Cost of swimming measured at optimum speed: scale effects, differences between swimming styles, taxonomic groups and submerged and surface swimming *Comput. Biochem. Physiol.* **97A** 91–9

Walker J A 2004 Kinematics and performance of maneuvering control surfaces in teleost fishes *IEEE J. Ocean. Eng.* **29** 572–84

Walker J A and Westneat M W 2000 Mechanical performance of aquatic rowing and flying *Proc. R. Soc. B* **267** 1875–81

Walker J A and Westneat M W 2002 Kinematics, dynamics, and energetics of rowing and flapping propulsion in fishes *Integr. Comput. Biol.* **42** 1032–43

Webb B 2001 Can robots make good models of biological behavior? *Behav. Brain Sci.* **24** 1033–50

Webb B 2002 Robots in invertebrate neuroscience *Nature* **417** 359–63

Webb P W 2004 Maneuverability—general issues *IEEE J. Ocean. Eng.* **29** 547–55

Webb P W 2006 Stability and maneuverability *Fish Biomechanics* vol 23 ed R E Shadwick and G V Lauder (New York: Elsevier) pp 281–332 (*Fish Physiology Series*)

Wyneken J 1997 Sea turtle locomotion: mechanics, behavior, and energetics *The Biology of Sea Turtles* ed P L Lutz and J A Musick (Boca Raton, FL: CRC Press) pp 165–98